https://doi.org/10.5194/egusphere-2023-2985
Preprint. Discussion started: 3 January 2024

Research of mechanical model based on characteristics of fracture mechanics of ice cutting for scientific drilling in polar region

Xinyu Lv[1, 3], Zhihao Cui[2, 3], Ting Wang[2], Yumin Wen[2], An Liu[4], Rusheng Wang[2, 3*]

[1] Naval Architecture and Ocean Engineering College, Dalian Maritime University, Dalian 116026, China.
[2] College of Construction Engineering, Jilin University, Changchun, 130021, China
[3] Polar Research Center, Jilin University, Changchun, 130021, China
[4] Power China Huadong Engineering Corporation Limited, Hangzhou, 310014, China

Correspondence: Rusheng Wang (wangrs@ jlu.edu.cn)

Abstract： Scientific drilling in polar regions plays a crucial role in obtaining ice cores and using them to understand climate change and to study the dynamics of the polar ice sheet and its impact on global environmental changes (sea level, ocean current cycle, atmospheric circulation, etc.). Mechanical rotary cutting is a widely used drilling method that drives the cutter to rotate to cut and drill through ice layers. It is necessary to conduct in-depth research on the brittle fracture behavior of ice and mechanical model, and analyze the factors and specific mechanisms (cutter's angle, rotation speed of the drill bit, and cutting depth) affecting cutting force for the rational design of ice-core drill system, improving the efficiency of ice-core drilling, and ensuring the drilling process smoothly. Therefore, in this paper, the process of ice cutting was observed, the fracture mechanics characteristics of ice cutting process wad analyzed, the formation process of ice chips was divided into three stages, and the mathematical model for the cutting force was established based on the observation results. It describes the damage conditions of ice failure and points out the influencing factors and specific influencing laws on cutting force. Furthermore, the cutting force generated under various experimental conditions was tested. Based on typical real-time data curves of cutting force, the characteristics of cutting force were analyzed during the cutting and drilling process. Based on the comparison results of the average cutting force, the influence mechanism of various parameters on the cutting force is obtained. This proves the correctness of the mathematical model of the cutting force and provides a theoretical reference for the calculation of cutting force during ice cutting and drilling in polar regions.

1. Introduction

https://doi.org/10.5194/egusphere-2023-2985
Preprint. Discussion started: 3 January 2024

As the largest cold source on Earth, Polar ice sheets/glaciers are an important component of the Earth's system related to the Earth's crust, glaciers, ice shelf, ocean, and atmosphere, it has a profound impact on global changes such as climate change and sea level rise et al (Lin Yang et al., 2023). Many scientific issues related to polar regions can be solved and validated by carrying out scientific drilling in ice sheets and obtaining ice cores (S.H. Faria et al., 2014; P. Talalay et al., 2015; P.L. Cao et al l., 2019). Mechanical rotary drills have been widely used in the field of polar ice core drilling (Ueda and Garfield, 1968, 1969; Gundestrup et al., 1984; Kudryashov et al., 1994; Stanford, 1992; Wumkes, 1994; Fujii et al., 1999; Takahashi et al.,2002; Johnsen et al., 2007; Shturmakov et al., 2007). The process of ice core drilling mainly consists of three steps: Cutting and drilling of the ice sheet, removal and transport of the ice chips generated at the hole bottom, and the collection of ice core and chips precipitation (Litvinenko VS and Nikolay I Vasiliev et al., 2014). These three steps are interrelated, and all of them have significant effects on the process of drilling. The cutting and drilling of the ice sheet generate a cutting force, which not only affects the selection of the motor system of the drill but also the design of the anti-torsion system, and even determines the success or failure of the cutting and drilling of the ice sheet. By conducting in-depth research on the fracture mechanics characteristics of solid ice, establishing a mechanical model for ice cutting, and determining the factors and specific mechanisms affecting cutting force, it can contribute to the rational design of the drilling tool system, the improvement of drilling efficiency, and ensure the smooth progress of drilling.

During ice core drilling, ice cutting is periodically carried out. At first, the moving cutters cut into the ice and compress it. When the level of stress near the edge of the cutter exceeds the cutting point, a crack is formed in the direction from the edge to the surface. This means that the horizontal force of cutting, called P_x, creates a repeated series of breaks, and its value is considered to be the mean force over the cutting length. Griffith (1920) assumed that when the energy of elastic strain exceeds the surface energy, the existing micro-crack starts to extend like an avalanche, and the materials break. Mellor and Sellman (1976) suggested that cutting force P_x can be calculated by using specific energy E_S (N/m^2), which is the energy consumed per unit of cutting volume:

$$P_x = bhE_S \quad (1)$$

where b is the width of the cutter; h is the depth of cut.

https://doi.org/10.5194/egusphere-2023-2985
Preprint. Discussion started: 3 January 2024

Using the formula (1) to calculate cutting force is difficult because specific energy is a vague concept. The formula ignores the influence of the structure of the cutter on the cutting force and lacks a certain degree of practicality. Due to the difficulty of conducting strict theoretical methods for the design of rock-cutting machines, many of the same experimental methods were developed by Mellor (1981). Maeno (1988) assumed that in any deformation process caused by compression, tension, bending, or cutting, the mechanics of ice failure are determined by the processes of inter/intragrain sliding. Taking the ideal monocrystal of ice, the theoretical stress needed for the formation of sliding zones is near 100 MPa, but for real ice, it does not exceed 0.1– 0.5 MPa (Lavrov, 1969). The contradiction is explained by the disposition theory. According to this theory, the deformation of the ice is determined by the defects which already exist in the ice crystal. The internal defects gradually expand under the action of external forces, the ice destruction occurs.

Research about the calculation of cutting resistance of soil and sand is abundant, however, most of which are empirical formulas based on an experimental basis (Jiang Pengnian, 1982). Due to the non-uniformity, hard brittle, and the factors that affect cutting resistance are complex, most studies on solid ice are conducted to investigate the influence of a certain variable on cutting resistance (Chiaia, 2008; S. Hell et al., 2014; A. Chao Correas et al., 2022). The in-depth study of the cutting properties of solid ice was rarely reported.

In this paper, images of the cutting and drilling process of the ice under various experimental conditions were captured, the fracture mechanics characteristics of the ice cutting process were analyzed, and the formation process of ice chips was clear and divided into three stages. Based on the result, a mechanics and mathematical model of ice cutting was built, and the influencing factors and specific influencing laws on cutting force were analyzed. Finally, the influencing factors and laws were verified through experimental tests. Which provides a theoretical reference for the calculation of cutting force during ice cutting and drilling.

2. Observation of ice fissure propagation in the process of ice cutting for ice-core drilling

2.1. Test stand design for study on ice cutting process

To observe the cutting and drilling process of the ice under various experimental conditions, an ice cutting and drilling simulation test stand has been designed (Fig. 1).

https://doi.org/10.5194/egusphere-2023-2985
Preprint. Discussion started: 3 January 2024

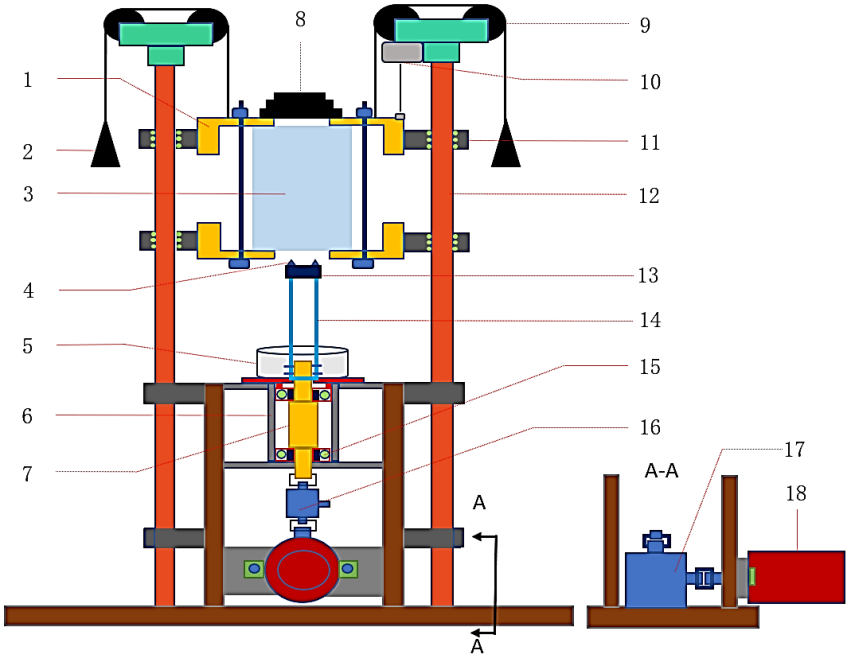

Figure 1. Schematic diagram of the experimental platform: 1-ice box; 2-balance weight 1; 3-ice block; 4-cutter; 5-ice chips collector; 6-cup set; 7-stepped shaft; 8-dead weight; 9-fixed pulley; 10-draw-wire displacement sensor; 11-slider; 12- slide rail; 13-drill bit; 14- drill pipe; 15- bearing; 16-torque sensor; 17- directional converter; 18-servo motor

To ensure the ice cutting and drilling proceed smoothly and the WOB is constant during the drilling process, the drilling direction is inverted upward. Therefore, the ice chips generated in the drilling process directly fall into the ice chips collector due to gravity, there will be no adhesion or blockage on the drill bit. During the experimental process, the ice block and ice box can slide nearly frictionless as they are connected to two parallel slide rails through four sliders, and the slider is equipped with rolling balls inside to ensure that the slider slides almost frictionless on the slide rail. So, during the drilling process, constant drilling pressure can be ensured, and multiple drilling pressure tests can be achieved by increasing or decreasing balance weight and dead weight. The drill pipe, drill bit, and cutters are driven to rotate by the servo motor system, and its rotation speed can be adjusted arbitrarily between 0-1000rpm. In this way, the adjustment of the rotation speed of the drill bit is achieved. The cutter equipped in the experimental test stand can be replaced arbitrarily according to the experimental requirements, therefore, it is possible to conduct cutting and drilling tests on cutters with various structures.

https://doi.org/10.5194/egusphere-2023-2985
Preprint. Discussion started: 3 January 2024

During the experiment, the torque generated by driving the rotation of drill pipes, step shafts, and other components, as well as the cutting torque generated by ice cutting is measured by the torque sensor. Before conducting the cutting and drilling experiment, adjust the rotation speed of the drill bit to the rotation speed for the next experiment, and let the drill bit and other components blank run. After the torque measured by the torque sensor stabilizes, the torque is recorded as T_1. Next, perform cutting and drilling. After the cutting and drilling process stabilizes, the recording of cutting torque begins. after the drilling process, the average cutting torque during this period is recorded as T_2. So, the torque for ice blocks cutting T_c can be calculated according to the following formula (2).

$$T_c = T_2 - T_1 \quad (2)$$

The drilling depth and time are measured by the Draw-wire displacement sensor. The formation process of ice chips is captured by a high-speed camera.

2.2. Test stand building and observation of ice fissure propagation during ice-core drilling testing

Based on the above working principle, the ice core drilling test stand has been established (Fig. 2).

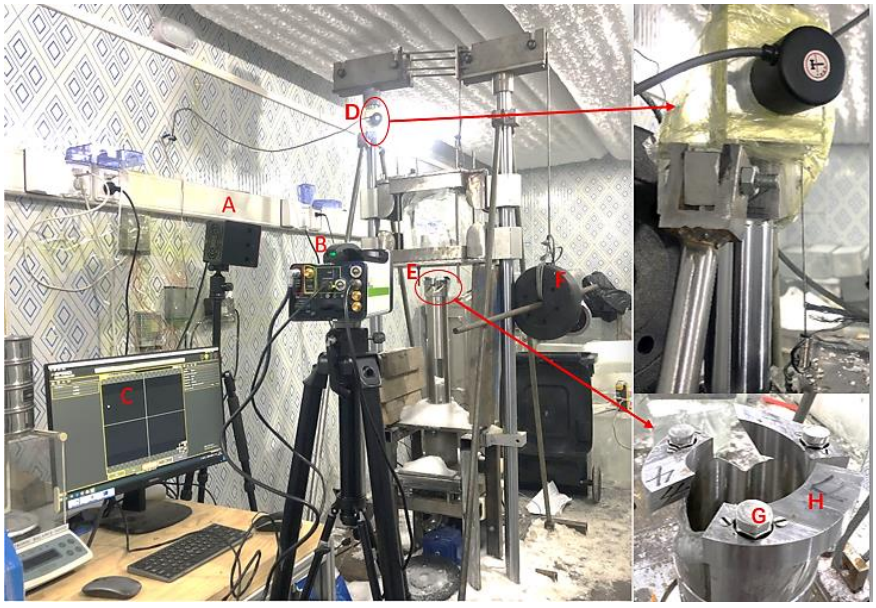

Figure 2. Test stand: A-light source; B-high speed camera; C-image display computer; D-draw-wire displacement sensor; E-drill bit; F-counterweight block; G-drill bit shoe; H-cutter

The specific parameters of the main equipment in the test stand are shown in Table 1.

https://doi.org/10.5194/egusphere-2023-2985
Preprint. Discussion started: 3 January 2024

Table 1. Main parameters of equipment

equipment and sensor		Model	Main parameters
Servo motor system	Driver	3DM2080-DSP	Drive voltage: 130-220VAC Pulse mode: Mono pulse Adjustment range: 0-1000rpm
	Motor	130BYG350D	Maximum output torque: 60N.M Step angle: 1.2° Rated voltage and current: 220V and 8.5A
	Pulse generator	CS10-3	Output mode： Steering + pulse Adjustment range: 0-1000rpm Output signal voltage: 5V; Power range:9-30V
Torque sensor		LLBLS-I	Measuring range: 60N.M: Overall accuracy:0.3% Maximum speed: 6000rpm
Draw-wire displacement sensor		MPS-M	Measuring distance:0-1500mm Resolving power:0.01mm; Pulling force of stay wire:4N
Slide rail and slider system		Ø50; SK50	Friction coefficient: 0.0010-0.0015
High-speed camera		Ispeed-7	Technology: CMOS active pixel Resolution: 2048×1536 Frames per second: 1000000fps Shutter: 1us Lens options: F mount/G mount/C mount

Before the experiment, the cutters (Fig.2.H) made from tool steel (W18Cr4V) shall be installed on the drill bit (Fig.2.E) through bolts and pins (Fig.2.H) that also serve as the shoes with adjustable height. The height of the bolts is lower than the height of the cutter's tip when the ice block slides into contact with the shoes, the cutters have been cut into the ice block at the designed depth. Thus, the cutting and drilling at the designed cutting depth is realized and the cutting depth has been accurately controlled.

Aiming the high-speed camera (Fig.2.B) at the cutting edge of the cutter, adjusting the frame number of the high-speed camera to 100,000, meanwhile, supplementing the light on the object with the light source (Fig.2.A), until the image displayed in the computer (Fig.2.C) is clear. After the experiment, the images of the formation process of ice chips are captured and saved in a high-speed camera. The observation experiment of the cutting and drilling process is conducted under various experimental conditions (multiple cutter angles, cutting depths, and rotation speed of drill bit). The specific parameters of experimental conditions are shown in Table 2. The cutters tested in the experiment are shown in Fig. 3.

https://doi.org/10.5194/egusphere-2023-2985
Preprint. Discussion started: 3 January 2024

Table 2. The specific parameters of experimental conditions

Structure of cutter						
Width (mm)	Rake angle (°)	Relief angle (°)	Cutting depth (mm)	Rotation speed (rpm)	Ice sample dimension (mm)	Ice core diameter (mm)
25	20	5	1	50	~250×250×450	60
	30	10	2	100		
	40	15	3	150		

Figure 3. Multi-group structure cutters

The ice blocks used in this experiment are frozen by an ice-making machine (Fig.4), which can produce transparent ice samples without bubbles. Then, we divided these blocks into experimental ice blocks with uniform dimensions (Fig.5) of ~250×250×450 mm. and all tests were carried out in the refrigerated container with a constant temperature of -15℃.

Figure 4. Ice-making machine

Figure 5. Experimental ice samples

3. Analysis of characteristics of ice fracture mechanics in the process of ice cutting

Under various experimental conditions, the ice cutting process is similar. It is preliminarily observed after the mechanical testing of ice under a special experimental condition (rake angle is 30°, relief angle

https://doi.org/10.5194/egusphere-2023-2985
Preprint. Discussion started: 3 January 2024

is 25°, cutting depth is 2mm and the rotation speed of the drill bit is 100 rpm). The actual ice-cutting process captured by a high-speed camera is shown in Fig. 6.

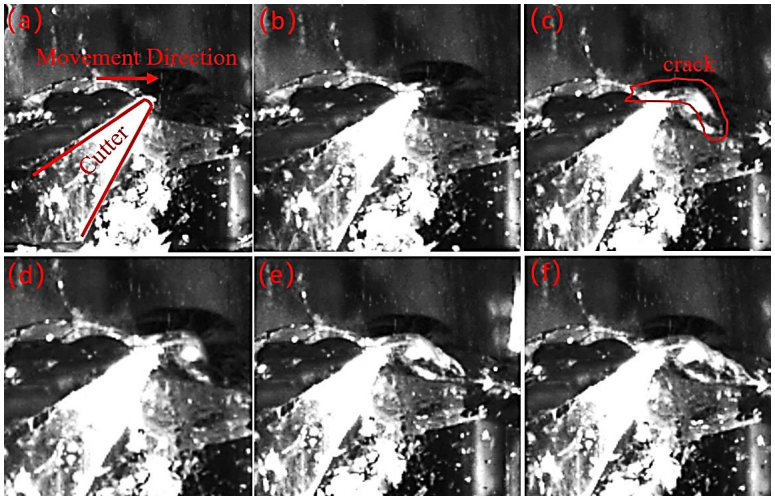

Figure 6. Cutting process captured by high-speed video camera

In the cutting process, the cutting of the ice is constantly repeated, the main damaged form of ice is a brittle fracture, the chips show wedge block, but the wedge itself does not significantly deform, and wedge-shaped ice chips with different particle sizes are constantly formed. The formation process of a single large particle of ice chips can be divided into three stages. In the first stage, the cutter invades the ice, and the ice is compressed by the rake and relief surfaces of the cutter, resulting in ice crushing and smaller ice chip formation (Fig. 6. a, b). In the second stage, with the rotation of the drill bit, cracks appeared in the ice, and the cracks began to expand along a direction that approximately presented an angle of 45° with the horizontal direction (Fig. 6. c, d). However, there were no gaps or separations between the ice and cutters on both sides of the cracks. In the third stage, the cutter moved forward, the crack expanded to form ice chips with large particle size that slid forward, and finally detached from the ice. At the same time, ice chips with small particle sizes were also generated on the sliding surface (Fig. 6. e, f).

4. Study on a mechanical model of ice cutting process

4.1. Mechanical model building based on the characteristics of ice fracture mechanics

According to the observation results of the ice cutting, it can be considered that the damage of the ice is the result of shear slip failure caused by the compression effect of the cutter. In this process, the force

https://doi.org/10.5194/egusphere-2023-2985
Preprint. Discussion started: 3 January 2024

exerted on the ice chips mainly includes the squeezing force F_n towards the ice, and along the normal direction of the cutter's rake face. The frictional force F_m exerted by the cutter when the ice chips flow out; At the same time, the shear surface of the ice will also be subjected to normal pressure F_{ns} and shear force F_s. Before the cutting of the ice, these two pairs of forces are in equilibrium. The relationships between these forces are analyzed in front of the cutting edge (Fig. 7).

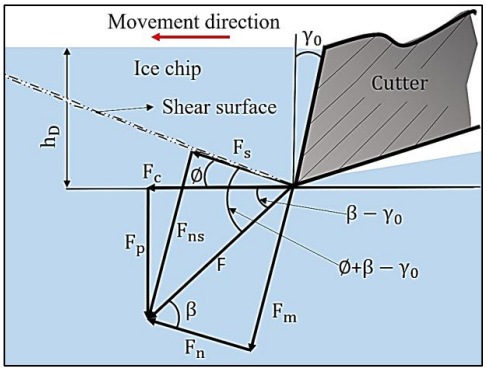

Figure 7. Relationship between force and angle

Where F is the combined force of F_m and F_n, $\emptyset$ is the shear angle, β (Friction angle) is the angle between F_n and F, γ_0 is the rake angle of the cutter, F_p is the component force perpendicular to the movement direction of the cutter, which is applied to the cutter and mainly provided by the weight on drill bit during the ice layer cutting and drilling, causing the cutter to cut into the ice to a certain depth. Where F_c is the component force acting on the ice layer, and during the ice layer cutting and drilling process, this force is mainly provided by the motor, which is called the cutting force. h_D is the cutting thickness.

If the cutting width is represented by b_D, The cutting width represents the width of the annular gap between the ice core and the hole wall in the process of ice drilling (cutting width, width of the cutter), The area of the nominal cross-section of the cutting layer is represented by A_D ($A_D = h_D b_D$), The area of shear surface is represented by A_s ($A_s = A_D/sin\emptyset$), the shear stress on the shear plane is represented by τ, then

$$F_s = \tau A_s = \frac{\tau A_D}{sin\emptyset} \quad (3)$$

According to Fig. 7, it can be concluded that:

$$F_s = F\cos(\emptyset + \beta - \gamma_0) \quad (4)$$

https://doi.org/10.5194/egusphere-2023-2985
Preprint. Discussion started: 3 January 2024

According to the relationship between various forces, it can be concluded that：

$$F = \frac{F_s}{\cos（\emptyset+\beta-\gamma_0）} = \frac{\tau A_D}{sin\emptyset\cos（\emptyset+\beta-\gamma_0）} \quad （5）$$

$$F_p = F\sin（\beta-\gamma_0） = \frac{\tau A_D \sin（\beta-\gamma_0）}{sin\emptyset\cos（\emptyset+\beta-\gamma_0）} \quad （6）$$

$$F_c = F\cos（\beta-\gamma_0） = \frac{\tau A_D \cos（\beta-\gamma_0）}{sin\emptyset\cos（\emptyset+\beta-\gamma_0）} \quad （7）$$

4.2. Analysis of factors influencing cutting forces via the mechanical model

According to Fig. 7, there is no shear stress in the plane perpendicular to the combined force F, so the main stress is completely determined by the F. The material is in the state of plane stress, and the included angle between the direction of the maximum shear stress and the direction of the maximum principal stress is 45°, the included angle between the maximum principal stress and the F is 45 °, then there is：

$$\emptyset + \beta - \gamma_0 = \frac{\pi}{4} \quad （8）$$

So：

$$\emptyset = \frac{\pi}{4} - \beta + \gamma_0 \quad （9）$$

The shear angle $\emptyset$ is affected by the rake angle of the cutter γ_0 and friction angle β. As the rake angle of the cutter γ_0 increases, the shear angle $\emptyset$ increases; as the friction angle β increases, $\emptyset$ decreases.

The area of the nominal cross-section of the cutting layer is represented by A_D ($A_D = h_D b_D$), The area of the shear surface is represented by A_s ($A_s = A_D/sin\emptyset$), the shear stress on the shear plane is represented by τ, then, according to equation (5) and the relationship between the nominal cross-section and the shear plane, it can be obtained that:

$$F_c = \frac{\tau A_D \cos（\beta-\gamma_0）}{sin\emptyset\cos（\emptyset+\beta-\gamma_0）} \quad （10）$$

When the ice is about to break, the shear stress on the shear plane reaches its maximum value. This value is determined by the properties of the ice and will not change as the drilling conditions. Therefore, the cutting force is influenced by the cutting width of the cutter and the cutting depth. The cutting force shows a linear increasing trend with the increase of the cutting width and the cutting depth. In addition, the cutting force is also affected by the shear angle $\emptyset$、friction angle β, and cutter's rake angle γ_0. The friction angle β is a certain value as the properties of the ice and cutter's material. The shear angle $\emptyset$ is determined by the friction angle and the cutter's rake angle as shown in formula (9). Substituting equation (9) into (10) and solving for the combined cutting force F_c, the following equation can be given:

https://doi.org/10.5194/egusphere-2023-2985
Preprint. Discussion started: 3 January 2024

$$F_c = \frac{\tau h_D b_D \cos(\beta-\gamma_0)}{\sin(\frac{\pi}{4}-\beta+\gamma_0)\cos(\frac{\pi}{4})} \quad (11)$$

After simplifying the above equation, it can be obtained that:

$$F_c = \frac{2\tau h_D b_D}{1-\tan(\beta-\gamma_0)} \quad (12)$$

It can be seen from the formula (12) that the factors affecting the cutting force mainly consist of four sides: The first aspect, it related to the shear strength of the ice, with the increase of shear strength, the cutting force increases gradually. The second aspect, it influenced by the cutting depth, with the increase of cutting depth, the cutting force increases gradually. The third aspect, it affected by the cutting width, with the increase of cutting width, the cutting force increases gradually. Finally, the rake angle of the cutter also has an impact on the cutting force. Formula (12) shows that: within the $\beta-\gamma_0 \le \frac{\pi}{2}$ range, as the rake angle of the cutter γ_0 increases, $\beta-\gamma_0$ gradually decreases, and the $\tan(\beta-\gamma_0)$ decreases, $1-\tan(\beta-\gamma_0)$ increases, F_c decreases.

5. Test on the characteristics of cutting force and its influencing factors for verifying the mechanical model

5.1 Analysis of the characteristics of cutting force

To verify the theoretical analysis results of the factors affecting cutting force, the cutting torque collected by the torque sensor under various cutter angles, rotation speed of the drill bit, and cutting depth conditions were measured.

After the experiment, the torque for ice cutting and drilling can be obtained through formula (2). The schematic diagram of the torque and cutting force generated during the ice cutting drilling process is shown in Figure 8, The relationship between the cutting force F_c generated by cutting the area of the circular ring and the torque T_c measured by the torque sensor is as follow.

$$T_c = F_c r_A \quad (13)$$

Where r_A is the average radius of the circular ring.

https://doi.org/10.5194/egusphere-2023-2985
Preprint. Discussion started: 3 January 2024

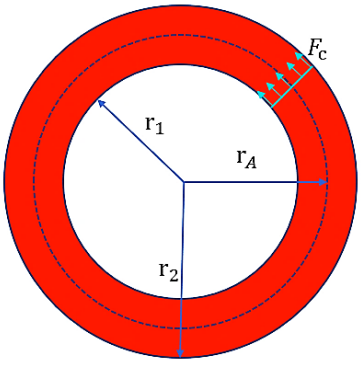

Figure 8. The schematic diagram of the torque and cutting force

By processing the data collected by the torque sensor, the cutting force generated by one cutter during the ice block cutting and drilling is obtained. The typical cutting force trace generated during the ice cutting process is shown in Fig. 9.

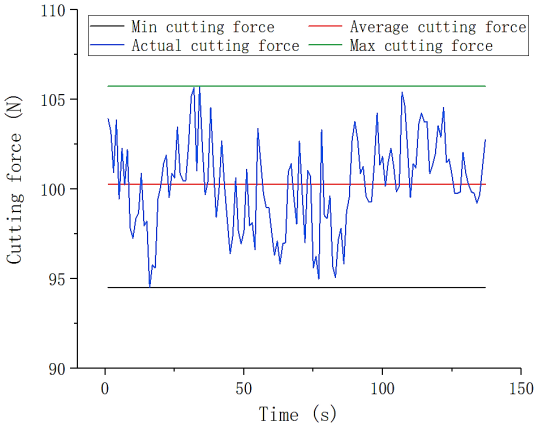

Figure 9. Typical cutting force trace（Cutting depth is 1mm; Rotation speed of drill bit is 50rpm; Rake angle is 30°; Relief angle is 5°）

During the ice core drilling, all cutting force traces fluctuate at a certain frequency within a certain range, and the fluctuation consists primarily of two frequencies. The higher frequency is related to the resolution of the sensor. The sensor outputs data at a certain interval during the recording process, the output data is not continuous, resulting in fluctuations in the trace. The lower frequency is related to the formation of large particle ice chips and should vary with the rotation speed of the cutter. As the cutter is pressed into the ice, the cutting force begins to rise. When the cutting force reaches the point required

https://doi.org/10.5194/egusphere-2023-2985
Preprint. Discussion started: 3 January 2024

for the ice layer to break, the ice layer undergoes shear-slip deformation, and ice chips form. Then, before the cycle repeats, the force suddenly decreases, the cutting force fluctuates, and the drill speed accelerates, the frequency of this cutting force fluctuation increases.

5.2. Test of the factors influencing cutting force

After the cutting and drilling experiments, the average cutting force was obtained under each experimental condition. Plots of the average cutting force versus the cutter's rake angle are shown in Fig. 10.

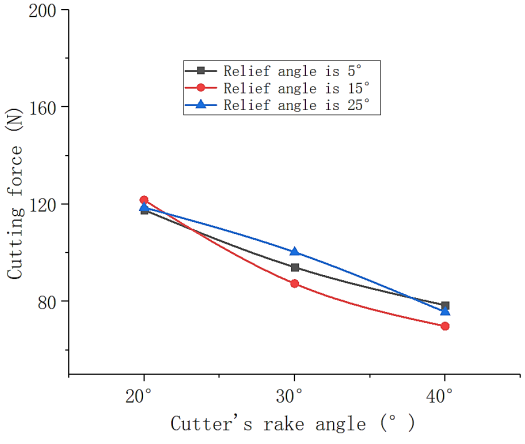

(a) The cutting depth is 1 mm, and the rotation speed of the drill bit is 100rpm

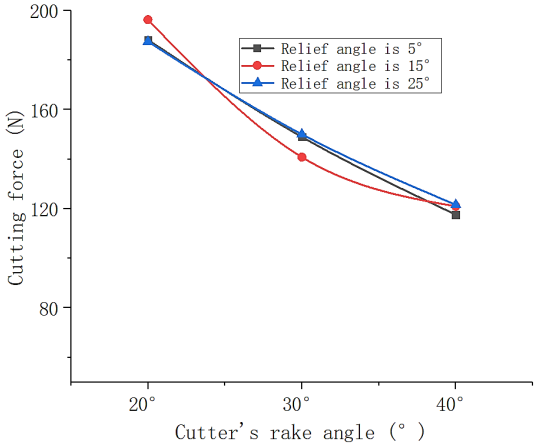

(b) The cutting depth is 2 mm, and the rotation speed of the drill bit is 100rpm

https://doi.org/10.5194/egusphere-2023-2985
Preprint. Discussion started: 3 January 2024

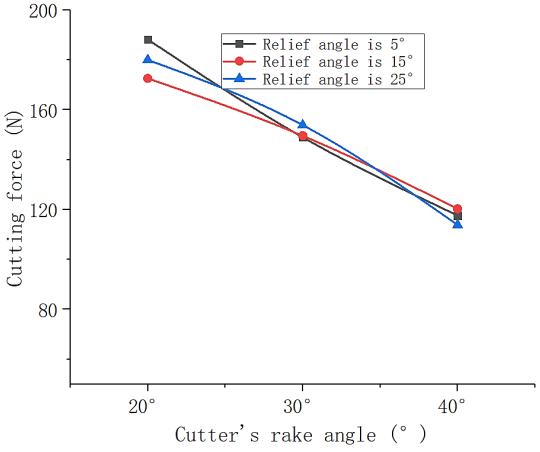

(c) The cutting depth is 2 mm, and the rotation speed of the drill bit is 50rpm

Figure 10. Cutting force versus cutter's rake angle

As shown in Fig. 10, when the cutting depth is 2mm, the rotation speed of the drill bit is 100 rpm, and the rake angle of the cutter is 20 °, the cutting force reaches the maximum value of 196.3451N. When the cutting depth is 1mm, the rotation speed of the drill bit is 100 rpm, and the rake angle of the cutter is 40 °, the cutting force reaches the minimum value of 69.83529N. The cutting force varies within this range under the other experimental conditions. That is, under various cutting depths and drill speed conditions, the cutting force gradually decreases with the increase of the cutter's rake angle.

Plots of the average cutting force versus the cutter's relief angle are shown in Fig. 11.

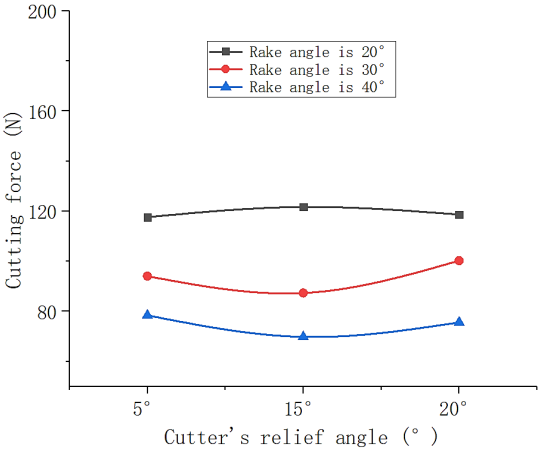

(a) The cutting depth is 1 mm, and the rotation speed of the drill bit is 100rpm

https://doi.org/10.5194/egusphere-2023-2985
Preprint. Discussion started: 3 January 2024

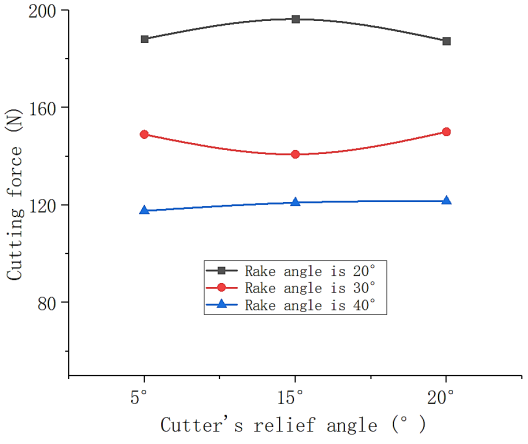

(b) The cutting depth is 2 mm, and the rotation speed of the drill bit is 100rpm

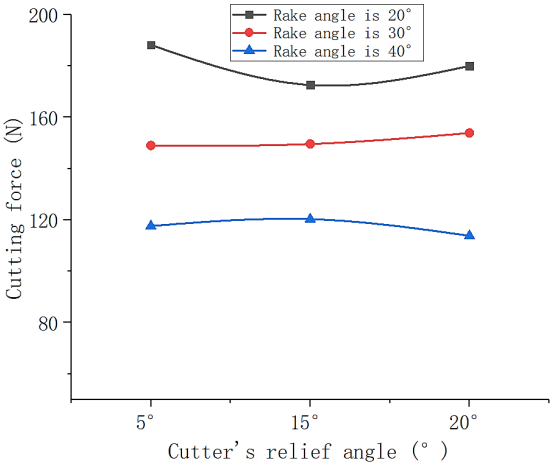

(c) The cutting depth is 2 mm, and the rotation speed of the drill bit is 50rpm

Figure 11. Cutting force versus cutter's relief angle

Under various experimental conditions, the relief angle of the cutter changes, and the cutting force only changes slightly. Moreover, with the change of the relief angle of the cutter, the cutting force does not show a clear and consistent change pattern. Therefore, it can be inferred that the relief angle of the cutter has no clear effect on the cutting force.

Plots of the average cutting force versus the rotation speed of the drill bit are shown in Fig. 12.

https://doi.org/10.5194/egusphere-2023-2985
Preprint. Discussion started: 3 January 2024

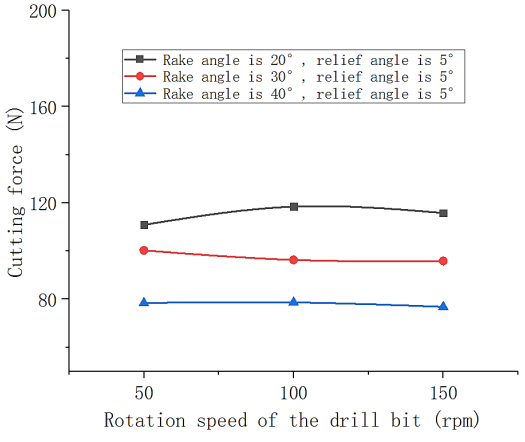

285

286

(a) The cutting depth is 1mm

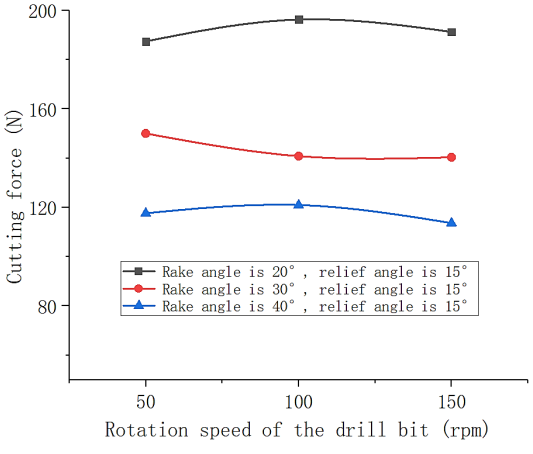

287

288

(b) The cutting depth is 2mm

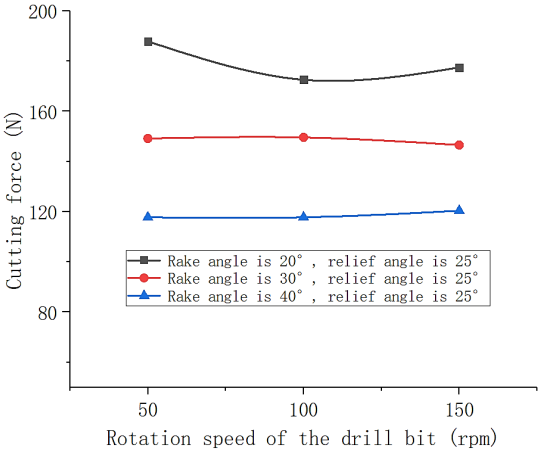

289

https://doi.org/10.5194/egusphere-2023-2985
Preprint. Discussion started: 3 January 2024

(c) The cutting depth is 2mm

Figure 12. Cutting force versus rotation speed of the drill bit

Under various experimental conditions, there is only a slight change in cutting force during the process of the rotation speed changing, and there is no clear pattern of change. The rotation speed of the drill bit does not affect the cutting force.

Plots of the average cutting force versus cutting depth are shown in Fig. 13.

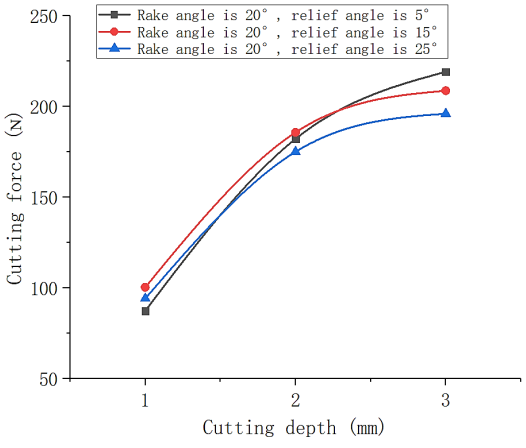

(a) The rotation speed of the drill bit is 50 rpm

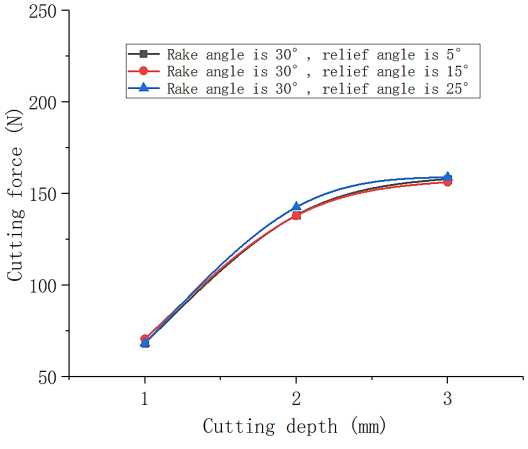

(b) The rotation speed of the drill bit is 100 rpm

https://doi.org/10.5194/egusphere-2023-2985
Preprint. Discussion started: 3 January 2024

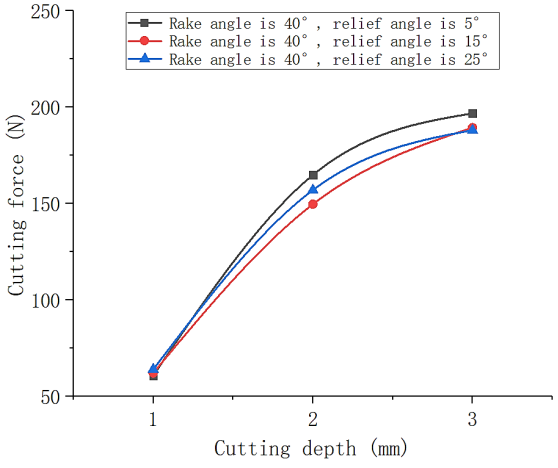

(c) The rotation speed of the drill bit is 100 rpm

Figure 13. Cutting force versus cutting depth

Under all experimental conditions, as the cutting depth increases, the cutting force shows a gradually increasing trend. When the cutting depth is 3mm, the maximum cutting force reaches 219.13725N. And, under the same experimental condition, the cutting depth increasing from 1 mm to 2 mm results in an approximate doubling of the cutting force. As the depth of penetration increases, the cutting force continues to increase, but the increasing trend gradually weakens.

6. Conclusions

It is preliminarily observed after the mechanical testing of ice, that the main damage form of ice is a brittle fracture in the cutting process. During this process, the cutters press into the ice to a certain depth and rotate, the ice withstands a squeezing effect from the rake face of the cutter and the shear slip deformation occurs. When the shear slip deformation reaches a certain degree, the ice undergoes shear failure and then forms ice chips. This process is constantly repeated throughout the cutting and drilling of the ice.

Based on the characteristics of ice cutting and the stress characteristics during the ice cutting and drilling process, a mechanical model of ice cutting was established. The mechanical model shows that the cutting force is not only affected by the mechanical properties of ice but also by the cutting width, cutting depth, and the rake angle of the cutter. As the cutting width and cutting depth increase, the cutting force increases; as the increase of rake angle of the cutter, the cutting force decreases. Additionally, the

https://doi.org/10.5194/egusphere-2023-2985
Preprint. Discussion started: 3 January 2024

characteristics of cutting force were analyzed through experimental methods, and we found that the cutting force fluctuated within a certain range. As the cutter is pressed into the ice, the cutting force begins to rise. When the cutting force reaches the point required for the ice layer to break, the ice layer undergoes shear-slip deformation, and ice chips form. Then, before the cycle repeats, the force suddenly decreases, and the cutting force fluctuates. Finally, the influencing factors and laws of cutting force were verified by analyzing the cutting force generated under various experimental conditions.

Date availability. No data sets were used in this article

Author contribution. Xinyu Lv: Conceptualization, Methodology, Writing – original draft; Zhihao Cui: Methodology, Validation, Formal analysis, Visualization; Ting Wang: Methodology, Validation, Formal analysis, Visualization; Yumin Wen: Conceptualization, Writing – review & editing, Methodology, Validation; An Liu: Methodology, Validation, Formal analysis, Visualization; Rusheng Wang: Methodology, Formal analysis, Supervision, Project administration, Funding acquisition.

Competing interests. The contact author has declared that neither of the authors has any competing interests.

Disclaimer. Publisher's note: Copernicus Publications remains neutral with regard to jurisdictional claims in published maps and institutional affiliations.

Special issue statement. This article is part of the special issue "Ice core science at the three poles (CP/TC inter-journal SI)". It is not associated with a conference.

Financial support. This paper presents research conducted with support from the National Key R&D Program of China (Project No. 2021YFA0719100; Subject No. 2021YFA0719103), and Jilin University "Interdisciplinary Integration and Innovation" project (Project No. 419021421601).

https://doi.org/10.5194/egusphere-2023-2985
Preprint. Discussion started: 3 January 2024

References

Lin Yang, Guangju Zhao, Xingmin Mu, Yanli Liu, Peng Tian, Puqiong, Danzengbandian, Historical and projected evolutions of glaciers in response to climate change in High Mountain Asia, Environmental Research, Volume 237, Part 2, 2023, 117037, ISSN 0013-9351. https://doi.org/10.1016/j.envres.2023.117037.

S.H. Faria, I. Weikusat, N. Azuma, The microstructure of polar ice. Part I: Highlights from ice core research[J], J. Struct. Geol. 61 (2014) 2–20. https://doi. org/10.1016/j.jsg.2013.09.010.

P. Talalay, C. Yang, P. Cao, et al., Ice-core drilling problems and solutions[J], Cold Reg. Sci. Technol. 120 (2015) 1–20. https://doi.org/10.1016/j.coldregions.2015.08.014.

P.L. Cao, H.Y. Cao, J.E. Cao, et al., Studies on pneumatic transport of ice cores in reverse circulation air drilling[J], Powder Technol. 356 (2019) 50–59. https://doi. org/10.1016/j.powtec.2019.08.001.

Ueda, H.T.,Garfirld, D.E.,1968. Drilling through the Greenland Ice Sheet. USA CRREL Spec.Rep., 126.Hanover.

Ueda, H.T.,Garfirld, D.E.,1969. Core Drilling through the Antarctic Ice Sheet. USA CREEL Tech, Rep., 231. Hanover.

Gundestrup, N.S., Johnson, S.J., Reeh, N., 1984. ISTUK: ADeep Ice Core Drill System. Proc. of the Second Int. Workshop/Symposium on Ice Drilling Technology. USA CREEL Spec. Rep., 84-34. Hanover, USA CREEL, pp. 7-19

Kudryashov, B.B., Vasiliv, N.L., Talalay, P.G., 1994, KEMS-112 Electromechanical ice core drill. Ice Drilling Technology, Proc. of the Fourth Int. Workshop on Ice Drilling Technology, Tokyo, April 20-23, 1993. Mem. Natl. Inst. Polar Res., 49, pp.138-152

Stanfors, K.l., 1992. An Engineering, Environmental, and Logistical Analysis of the Polar Ice Coring Office 13.2-cm Ice Coring System. PICO Rep. CP-92-2

Wumkes, M.A., 1994. Development of the U.S. Deep Coring Ice Drill. Ice Drilling Technology, Proc. of the Fourth Int. Workshop on Ice Drilling Technology, Tokyo, April 20-23, 1993.Mem. Natl. Inst. Polar Res., 49, pp.41-45.

Fujii, Y., Azuma, N., Tanaka, Y., Takahashi, A., Shinbori, K., Motoyama, H., Katagiri, K., Fujita, SH.,Miyahara, M., Nakayama, Y., Kameda, T., Saito, T., Saito, T., Shoji H., Shiraiwa, T., Narita, H., Kamiayma, K., Furukawa, T., Maeno, H., Enomoto, H., Naruse, R., Yokoyama, K., Hondo, T., Aageta, Y., Kawada, K., Watanabe, O., 1999. Deep ice coring at Dome Fuji station, Antarct. Rec. 43 (1), 162-210 (In Japanese).

Takahashi, A., Fujii, Y., Azuma, N., Motoyama, H., Shinbori, K., Tanaka, Y., Narita, H., Nakayama, Y., Kameda, T., Fujita, S., Furukawa, T., Takata, M., Miyahara, M., Watanabe, O., 2002.Improvements to the JARE deep ice core drill. Ice Drilling Technology, Proc. of the Fifth Int. Workshop on Drilling Technology, Nagaoka, 30 October-1 November 2000.Mem. Natl. Inst. Polar Res., 56, pp. 117-125.

Johnson, J.A., Mason, W.P., Shturmakov, A.J., Haman, S.T., Sendelbach, P.J., Mortensen, N.B., Augustin, L.J., Dahnert, K.R., 2007. A new 122mm electromechanical drill for deep ice-sheet coring (DISC): 5. Experience during Greenland field testing. Ann. Glaciol. 47, 54-60

https://doi.org/10.5194/egusphere-2023-2985
Preprint. Discussion started: 3 January 2024

Shturmakov, A.J., Lebar, D.A., Mason, W.P., Bentley, C.R., 2007. A new 122mm electromechanical drill for deep ice-sheet coring (DISC): 1. Design concepts. Ann.Glaciol. 47, 28-34.

Litvinenko VS, Nikolay I Vasiliev, Volodya Ya Lipenkov, Dmitriev AN, Podoliak AV (2014). Special aspects of ice drilling and results of 5G hole drilling at Vostok station, Antarctica. Annals of Glaciology, 55, 68, 173-178. https://doi: 10.3189/2014AoG68A040.

Mellor, M., Sellman, P.V., 1976. General consideration for drill system design. Ice-Core Drilling. Proc. of the Symp., Univ. of Nebraska, Lincoln, USA, 28–30 Aug. 1974. University of Nebraska Press, Lincoln, pp. 77–111.

Mellor, M., 1981. Mechanics of cutting and boring: Part 7. Dynam78 P.G. Talalay / Cold Regions Science and Technology 37 (2003) 69–79. https://doi:10.1016/S0890-6955(02)00276-6

Maeno, N., 1988. Nauka o l'de (Science About Ice). Mir, Moscow. Text in Russian, 231 pp.

Lavrov, V.V., 1969. Deformatsia i prochnost' l'da (Deformation and Strength of Ice). Gidrometeoizdat, Leningrad. Text in Russian, 208 pp.

Jiang Pengnian. Constitutive relations of Soil[M]. Beijing:Science Press,1982.

Chiaia., 2008. Triggering of dry snow slab avalanches: stress versus fracture mechanical approach [J]. Cold Regions Science and Technology,2008,53:170–178. https://doi:10.1016/j.coldregions.2007.08.003

S. Hell, P. Weißgraeber, J. Felger, W. Becker, A coupled stress and energy criterion for the assessment of crack initiation in single lap joints: A numerical approach, Engineering Fracture Mechanics, Volume 117, 2014, Pages 112-126, ISSN 0013-7944. https://doi.org/10.1016/j.engfracmech.2014.01.012.

A. Chao Correas, P. Cornetti, M. Corrado, A. Sapora, Dynamic crack initiation by Finite Fracture Mechanics, Procedia Structural Integrity, Volume 42, 2022, Pages 952-957, ISSN 2452-3216. https://doi.org/10.1016/j.prostr.2022.12.120